

MIT Open Access Articles

Improving product yields on D-glucose in Escherichia coli via knockout of pgi and zwf and feeding of supplemental carbon sources

The MIT Faculty has made this article openly available. **Please share** how this access benefits you. Your story matters.

Citation: Shiue, Eric, Irene M. Brockman, and Kristala L. J. Prather. "Improving Product Yields on D-Glucose in Escherichia Coli via Knockout of Pgi and Zwf and Feeding of Supplemental Carbon Sources." *Biotechnol. Bioeng.* (November 2014): n/a–n/a.

As Published: <http://dx.doi.org/10.1002/bit.25470>

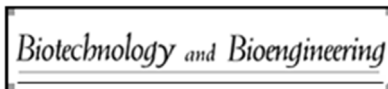
Publisher: Wiley Blackwell

Persistent URL: <http://hdl.handle.net/1721.1/92434>

Version: Original manuscript: author's manuscript prior to formal peer review

Terms of use: Creative Commons Attribution-Noncommercial-Share Alike





Improving Product Yields on D-Glucose in Escherichia coli via Knockout of *pgi* and *zwf* and Feeding of Supplemental Carbon Sources

Journal:	<i>Biotechnology and Bioengineering</i>
Manuscript ID:	14-568.R1
Wiley - Manuscript type:	Article
Date Submitted by the Author:	n/a
Complete List of Authors:	Shiue, Eric; MIT, Chemical Engineering Brockman, Irene; MIT, Chemical Engineering Prather, Kristala; MIT, Chemical Engineering;
Key Words:	Product yield, Strain engineering, Biomass, D-glucaric acid, Metabolic engineering

SCHOLARONE™
Manuscripts

View

1
2
3 **1 Improving Product Yields on D-Glucose in *Escherichia coli* via Knockout of *pgi* and *zwf***
4
5 **2**
6 **and Feeding of Supplemental Carbon Sources**
7

8
9 **3 Eric Shiue, Irene M. Brockman, and Kristala L. J. Prather***
10

11
12 *Department of Chemical Engineering*
13

14
15 *Synthetic Biology Engineering Research Center (SynBERC)*
16

17
18 *Massachusetts Institute of Technology*
19

20
21 *Cambridge, MA 02139, USA*
22
23

24
25 **8**
26
27
28 **9 * Corresponding author:**
29

30
31 **10 Department of Chemical Engineering**
32

33
34 **11 77 Massachusetts Avenue**
35

36
37 **12 Room E17-504G**
38

39
40 **13 Cambridge, MA 02139**
41

42
43 **14 Phone: 617.253.1950**
44

45
46 **15 Fax: 617.258.5042**
47

48
49 **16 Email: kljp@mit.edu**
50

51
52 **17 Running title: Improved product yields on glucose in *E. coli***
53

54
55
56
57
58
59
60

1
2
3 19 **Abstract**
4
5

6 20 The use of lignocellulosic biomass as a feedstock for microbial fermentation processes presents
7
8 21 an opportunity for increasing the yield of bioproducts derived directly from glucose.

9
10 22 Lignocellulosic biomass consists of several fermentable sugars, including glucose, xylose, and
11
12 23 arabinose. In this study, we investigate the ability of an *E. coli* Δpgi Δzwf mutant to consume
13
14 24 alternative carbon sources (xylose, arabinose, and glycerol) for growth while reserving glucose
15
16 25 for product formation. Deletion of *pgi* and *zwf* was found to eliminate catabolite repression as
17
18 26 well as the ability of *E. coli* to consume glucose for biomass formation. In addition, the yield
19
20 27 from glucose of the bioproduct D-glucaric acid was significantly increased in a Δpgi Δzwf strain.
21
22
23
24
25

26 28
27
28
29 29 **Keywords**
30

31
32 30 Product yield
33
34

35
36 31 Strain engineering
37
38

39 32 Biomass
40
41

42 33 D-glucaric acid
43
44

45 34
46
47
48
49
50
51
52
53
54
55
56
57
58
59
60

1. Introduction

In recent years, concerns over declining petroleum reserves and climate change due to atmospheric carbon dioxide accumulation have spurred significant interest in using alternative feedstocks for the manufacture of petroleum-derived products. Because it is renewable and abundant, non-food plant (lignocellulosic) biomass represents a promising alternative feedstock to crude oil. Moreover, because plants assimilate carbon dioxide during growth, the use of plant-based feedstocks could potentially slow the accumulation of carbon dioxide in the atmosphere. Recent research has focused heavily on the identification of ideal plant biomass feedstocks (Joyce and Stewart, 2012), the determination of commercially valuable, biomass-derived products (Werpy and Petersen, 2004), and the development of processes for converting plant biomass into these products of interest.

One such process that has received heavy attention is microbial fermentation. A significant portion of lignocellulosic biomass consists of fermentable sugars such as glucose, xylose, arabinose, and galactose (Joyce and Stewart, 2012), and many microbes are naturally able to convert these sugars into products of interest such as **biochemicals** and biopolymers (Lee, 1996). In addition, microbes can be engineered to produce a wide array of non-natural products via recombinant DNA technology (Curran and Alper, 2012). A few products, including D-glucaric acid (Moon et al., 2009) and D-gluconic acid (Rogers et al., 2006), are derived directly from glucose; however, microbial production of these products generally suffers from low yields, as a portion of the glucose feed is utilized to generate cell biomass. **For products such as these that do not require further glucose metabolism through the canonical reduction pathways, eliminating the ability to utilize glucose for growth may address this limitation.** We **thus** set out to design an

1
2
3
4 57 *E. coli* production platform that utilizes an alternative carbon source such as arabinose or xylose
5
6 58 for cell growth, reserving glucose solely for product generation to maximize yield.

7
8 59 The main pathways for glucose utilization in *E. coli* are depicted in Figure 1. Glucose enters
9
10 60 the cell through the phosphotransferase system (PTS) encoded by *ptsG* and *ptsHI-crr* and is
11
12 61 phosphorylated to glucose-6-phosphate in the process. Glucose-6-phosphate can then proceed
13
14 62 through the Entner-Dudoroff Pathway via *zwf* or through the Embden-Meyerhoff-Parnas
15
16 63 Pathway via *pgi*. The carbon in glucose-6-phosphate can also be stored as glycogen via *pgm*.
17
18 64 Previous work to engineer *E. coli* for co-utilization of glucose and alternative carbon sources
19
20 65 involved deleting the PTS system (Balderas-Hernández et al., 2011; Solomon et al., 2013; Wang
21
22 66 et al., 2011). By eliminating the PTS system, catabolite repression can be eliminated, allowing
23
24 67 simultaneous uptake of glucose and a secondary carbon source. However, these strategies also
25
26 68 eliminate *E. coli*'s primary method of glucose uptake, and the cell must rely on nonspecific
27
28 69 transporters to import glucose into the cell. Subsequent phosphorylation of glucose to glucose-6-
29
30 70 phosphate via ATP-dependent *glk* is also required for glucose metabolism in PTS-deficient *E.*
31
32 71 *coli*. Overexpression of the galactose:H⁺ symporter *galP* and upregulation of *glk* has been
33
34 72 shown to recover wild-type growth rates in PTS-deficient strains of *E. coli* (Hernández-Montalvo
35
36 73 et al., 2003). However, because glycolytic pathways remain intact in this strain, it is likely that
37
38 74 product yields on glucose would remain low. In this study, we explore the behavior of an *E. coli*
39
40 75 strain which lacks *pgi* and *zwf* and investigate this strain's ability to produce a glucose-derived
41
42 76 product when supplemented with L-arabinose and D-xylose, sugars which are readily available
43
44 77 from biomass. Glycerol is also explored as a carbon source, as its price has dropped significantly
45
46 78 in recent years due to significant increases in biodiesel production (Johnson and Taconi, 2009).
47
48 79 Previous work has demonstrated improved yield of glucose-derived products in a $\Delta pgi \Delta zwf$
49
50
51
52
53
54
55
56
57
58
59
60

1
2
3 80 strain supplemented with mannitol (Kogure et al., 2007; Pandey et al., 2013); however, the price
4
5
6 81 of mannitol remains high relative to glycerol and biomass-derived sugars.
7
8

9 82 **Materials and Methods**

10 11 12 83 **2.1 *E. coli* strains and plasmids**

13
14
15 84 *E. coli* strains, plasmids, and oligonucleotides used in this study are listed in Table I. All
16
17
18 85 molecular biology manipulations were performed according to standard practices (Sambrook and
19
20 86 Russell, 2001). *E. coli* DH10B was used for transformation of cloning reactions and propagation
21
22
23 87 of all plasmids. Strains M2, M2-2, and M3 were constructed by our group previously
24
25 88 (Gonçalves et al., 2013; Shiue and Prather, 2014). Strain M2 was generated via knockout of
26
27 89 *endA* and *recA* from *E. coli* MG1655. Strain M2-2 was generated via knockout of *gudD* and
28
29 90 *uxaC* from strain M2 to prevent consumption of D-glucaric and D-glucuronic acids during D-
30
31 91 glucaric acid production experiments. Strain M3 was derived from strain M2 via knockout of *pgi*
32
33 92 and served as an intermediate strain; this strain was not further characterized in this work.
34
35
36 93 Deletion of *zwf* from strain M3 was achieved by P1 transduction with Keio collection strain
37
38 94 JW1841-1 as the donor (Baba et al., 2006). The λ DE3 lysogen was then integrated site-
39
40 95 specifically into this quadruple knockout strain using a λ DE3 Lysogenization Kit (Novagen,
41
42 96 Darmstadt, Germany), generating strain M4 (MG1655(DE3) $\Delta endA \Delta recA \Delta pgi \Delta zwf$. To
43
44 97 prevent *E. coli* from consuming D-glucuronic and D-glucaric acids, both *gudD* and *uxaC* were
45
46 98 deleted from the genome. Deletion of *uxaC* was performed with λ -Red mediated recombination
47
48 99 (Datsenko and Wanner, 2000) using pKD46recA (Solomon et al., 2013). PCR primers
49
50 100 pKD13_uxaC_fwd and pKD13_uxaC_rev (Table 1) were used to amplify the recombination
51
52 101 cassette from pKD13 (Datsenko and Wanner, 2000), and strain M4 harboring pKD46recA was
53
54
55
56
57
58
59
60

1
2
3 102 transformed with this PCR product. The *kan* selection cassette was cured from successful
4
5 103 deletion mutants using FLP recombinase expressed from pCP20, generating strain M5. **Similar to**
6
7
8 104 **strain M3, strain M5 served as an intermediate strain only and was not further characterized in**
9
10 105 **this work.** Finally, strain M6 (MG1655(DE3) $\Delta endA \Delta recA \Delta pgi \Delta zwf \Delta uxaC \Delta gudD$) was
11
12 106 generated using the same λ -Red mediated recombination method described above; in this case,
13
14 107 primers pKD13_gudD_fwd and pKD13_gudD_rev were used to amplify the recombination
15
16 108 cassette from pKD13. pRSFD-IN and pTrc-Udh were constructed by our group previously
17
18 109 (Moon et al., 2009; Yoon et al., 2009). To construct pRSFD-IN-Udh, pRSFD-IN was first
19
20 110 digested with XhoI, end-filled with Klenow enzyme, then digested with EcoRI-compatible MfeI.
21
22 111 pTrc-Udh was then digested with EcoRI and SmaI, and the Udh-containing fragment was ligated
23
24 112 into digested pRSFD-IN to generate pRSFD-IN-Udh.
25
26
27
28
29

30 113 **2.2 Culture conditions**

31
32
33 114 For determination of growth curves, cultures were grown in 250 mL baffled shake flasks
34
35 115 containing 50 mL LB medium supplemented with approximately 10 g/L D-glucose, L-arabinose,
36
37 116 glycerol, and/or D-xylose as indicated in Figures 2-5. Seed cultures were grown overnight at
38
39 117 30°C and inoculated to an optical density at 600 nm (OD_{600}) of 0.005. Cultures were incubated
40
41 118 at 30°C, 250 rpm, and 80% relative humidity for 72 hours. To construct a growth curve, cell
42
43 119 densities were measured at regular time intervals on a DU800 Spectrophotometer (Beckman
44
45 120 Coulter, Pasadena, CA), with more frequent sampling during the exponential growth phase. For
46
47 121 analysis of metabolite concentrations, samples were taken daily, centrifuged to remove cell
48
49 122 debris, and the supernatants analyzed via high performance liquid chromatography as described
50
51 123 in Section 2.3.
52
53
54
55
56
57
58
59
60

1
2
3 124 For glucaric acid production in rich medium, cultures were grown in 250 mL baffled shake
4
5
6 125 flasks containing 50 mL LB medium supplemented with 10 g/L D-glucose and 10 g/L L-
7
8 126 arabinose, 10 g/L glycerol, or 10 g/L D-xylose. Cultures were induced at inoculation with 0.1
9
10 127 mM β -D-1-thiogalactopyranoside (IPTG). Ampicillin (100 μ g/mL) and kanamycin (30 μ g/mL)
11
12 128 were added for plasmid maintenance. Seed cultures were grown overnight at 30°C in LB
13
14 129 medium supplemented with 10 g/L D-glucose and 10 g/L L-arabinose, 10 g/L glycerol, or 10 g/L
15
16 130 D-xylose and inoculated to an OD_{600} of 0.005. Cultures were incubated at 30°C, 250 rpm, and
17
18 131 80% relative humidity for 72 hours. Adequate aeration for product formation was ensured with
19
20 132 the use of baffled shake flasks. Samples were taken daily, centrifuged to remove cell debris, and
21
22 133 the supernatants analyzed for metabolite concentrations.
23
24
25
26

27 134 For minimal medium experiments, a modified MOPS-buffered medium was used containing
28
29 135 10 g/L D-glucose, 6 g/L L-arabinose, 6 g/L NH_4Cl , 0.4 g/L K_2HPO_4 , 2 mM $MgSO_4$, 0.1 mM
30
31 136 $CaCl_2$, 40 mM MOPS, 4 mM tricine, 50 mM NaCl, 100 mM Bis-Tris, 134 μ M EDTA, 31 μ M
32
33 137 $FeCl_3$, 6.2 μ M $ZnCl_3$, 0.76 μ M $CuCl_2$, 0.42 μ M $CoCl_2$, 1.62 μ M H_3BO_3 , 0.081 μ M $MnCl_2$,
34
35 138 carbenicillin (100 μ g/mL), and kanamycin (30 μ g/ml). Seed cultures were started using a 1:100
36
37 139 dilution from LB and were grown at 30°C for 48 hours in modified MOPS. Working cultures
38
39 140 were inoculated to an OD_{600} of 0.02 and induced 32 hours after inoculation with 0.1 mM IPTG.
40
41 141 Cultures were incubated at 30°C, 250 rpm, and 80% relative humidity for 110 hours. Adequate
42
43 142 aeration for product formation was ensured with the use of baffled shake flasks. Samples were
44
45 143 taken periodically, centrifuged to remove cell debris, and the supernatants analyzed for
46
47 144 metabolite concentrations.
48
49
50
51
52

53 145 2.3 Determination of metabolite concentrations

54
55
56
57
58
59
60

1
2
3
4 146 D-glucose, L-arabinose, glycerol, D-xylose, and D-glucaric acid were quantified from
5
6 147 culture supernatants using high performance liquid chromatography (HPLC) on an Agilent
7
8 148 Series 1100 or Series 1200 instrument equipped with an Aminex HPX-87H column (300 mm by
9
10 149 7.8 mm; Bio-Rad Laboratories, Hercules, CA). Sulfuric acid (5 mM) was used as the mobile
11
12 150 phase at 35°C and a flow rate of 0.6 mL/min in isocratic mode. Compounds were detected and
13
14 151 quantified from 10 μ L sample injections using refractive index and diode array detectors.
15
16 152 Reported metabolite concentrations are the average of triplicate samples, and error bars represent
17
18 153 one standard deviation above and below the mean value.
19

22 154 3. Results

23
24 155 In *E. coli*, glucose is imported into the cell and phosphorylated to glucose 6-phosphate (G6P)
25
26 156 by the phosphotransferase system (PTS). Glucose metabolism then proceeds through two routes
27
28 157 (Figure 1): the Embden-Meyerhoff-Parnas Pathway via phosphoglucose isomerase (*pgi*) or the
29
30 158 Entner-Dudoroff Pathway via glucose 6-phosphate dehydrogenase (*zwf*). A third route
31
32 159 interconverts glucose 6-phosphate and glucose 1-phosphate via phosphoglucomutase (*pgm*) for
33
34 160 glycogen storage and accumulation, though flux through this node is typically extremely low
35
36 161 (Chassagnole et al., 2002). To eliminate native consumption of glucose, both *pgi* and *zwf* were
37
38 162 deleted from an MG1655-derived strain. Growth on M9 minimal medium supplemented with
39
40 163 various carbon sources confirmed that the $\Delta pgi \Delta zwf$ mutant does not grow on glucose but
41
42 164 retains the ability to utilize other carbon sources (Supplementary Figures 1 and 2).
43
44
45
46
47

48 165 3.1 Behavior of a $\Delta pgi \Delta zwf$ mutant

49
50 166 Cell growth was compared for strains M2 and M4, a $\Delta pgi \Delta zwf$ mutant in rich medium
51
52 167 supplemented with various carbon sources (Figure 2). Maximum specific growth rates for each
53
54 168 combination of strain and carbon supplement were also calculated (Table II). As expected,
55
56
57
58
59
60

1
2
3 169 growth of strain M2 was similar for all conditions tested, with similar lag phases and maximum
4
5 170 specific growth rates. Final cell densities were lower when strain M2 was fed D-glucose, likely
6
7
8 171 due to increased production of acetate (Figure 3), which has been shown to inhibit cell growth
9
10 172 (Roe et al., 1998). Growth of strain M4 was also similar for all conditions tested with the
11
12 173 exception of glycerol-supplemented cultures, which displayed a significant lag in growth of
13
14 174 approximately 24 hours. We hypothesize that this lag corresponds to depletion of the metabolic
15
16 175 precursors provided by LB and a metabolic shift towards gluconeogenic metabolism for growth
17
18 176 on glycerol. Maximum growth rate, lag time, and final cell densities are similar for strain M4 in
19
20 177 the presence of L-arabinose, glycerol, and D-xylose regardless of whether D-glucose was
21
22 178 supplemented in the growth medium, indicating that substrate consumption was similar in the
23
24 179 presence or absence of D-glucose. Overall, maximum growth rates of strain M4 were
25
26 180 approximately 70% that of strain M2.
27
28
29
30

31
32 181 Concentrations of D-glucose, alternative carbon source, and acetate were measured for each
33
34 182 strain/carbon supplement combination as a function of time (Figure 3). As expected, the
35
36 183 presence of D-glucose prevents consumption of the alternative carbon source in strain M2 via
37
38 184 catabolite repression. In contrast, the deletion of *pgi* and *zwf* prevents consumption of D-glucose
39
40 185 in strain M4. Interestingly, deletion of *pgi* and *zwf* appears to eliminate catabolite repression in
41
42 186 strain M4, as the presence of D-glucose does not preclude consumption of the alternative carbon
43
44 187 source in this strain.
45
46
47

48 188 This phenomenon is perhaps due to intracellular buildup of glucose-6-phosphate. Catabolite
49
50 189 repression is mediated by cyclic AMP (cAMP), which is synthesized by adenylate cyclase.
51
52 190 Adenylate cyclase is activated via phosphorylation by EIIA^{Glc}, but this phosphorylation can only
53
54 191 occur if EIIA^{Glc} has a phosphate group to donate. When glucose is being actively imported
55
56
57
58
59
60

1
2
3 192 through the PTS system, EIIA^{Glc} donates its phosphate to the incoming glucose, resulting in a
4
5
6 193 mostly unphosphorylated population of EIIA^{Glc}, inactive adenylate cyclase, and a low
7
8 194 concentration of cAMP. The absence or depletion of glucose from the culture medium leads to a
9
10
11 195 buildup of phosphorylated EIIA^{Glc}, activation of adenylate cyclase, and an increase in cAMP
12
13 196 concentration, eventually leading to the expression of catabolite-repressed genes such as *araBAD*
14
15 197 and *xyLAB*, which are important for arabinose and xylose metabolism, respectively. Thus,
16
17 198 catabolite repression occurs when there is active glucose flux into the cell, not simply when
18
19
20 199 glucose is present in the medium. In a $\Delta pgi \Delta zwf$ mutant, the accumulation of glucose-6-
21
22 200 phosphate quickly eliminates glucose flux into the cell, resulting in derepression of genes
23
24
25 201 normally repressed in the presence of glucose.

26 27 202 **3.2 D-glucaric acid production in a $\Delta pgi \Delta zwf$ mutant**

28
29 203 D-glucaric acid, a dicarboxylic organic acid, is a naturally occurring product which has been
30
31 204 investigated for a variety of potential applications. A biosynthetic pathway to D-glucaric acid
32
33
34 205 from D-glucose has been constructed in *E. coli* (Moon et al., 2009). This pathway begins with
35
36 206 glucose-6-phosphate, which is converted to *myo*-inositol-1-phosphate by *myo*-inositol-1-
37
38 207 phosphate synthase (INO1). *Myo*-inositol-1-phosphate is then dephosphorylated by an
39
40 208 endogenous phosphatase to yield *myo*-inositol, which is oxidized to D-glucuronic acid by *myo*-
41
42 209 inositol oxygenase (MIOX). Finally, D-glucuronic acid is oxidized to D-glucaric acid by uronate
43
44 210 dehydrogenase (Udh). Because production of D-glucaric acid requires glucose-6-phosphate, we
45
46 211 hypothesized that the yield of D-glucaric acid could be increased significantly in a $\Delta pgi \Delta zwf$
47
48 212 strain.

49
50
51
52
53 213 In supplemented LB, D-glucaric acid yield on glucose is increased in the $\Delta pgi \Delta zwf$ mutant
54
55 214 nearly 18-fold over an unmutated control supplemented with L-arabinose or D-xylose, while
56
57
58
59
60

1
2
3 215 yield is increased approximately 9-fold in the $\Delta pgi \Delta zwf$ strain supplemented with glycerol
4
5 216 (Table III). Additionally, D-glucaric acid titers are significantly higher in the $\Delta pgi \Delta zwf$ mutant
6
7 217 (Figure 4 and Table III). We hypothesize that deletion of *pgi* and *zwf* results in higher glucose-6-
8
9 218 phosphate pools, allowing INO1 to operate much closer to its maximum activity, which leads to
10
11 219 increased flux through the D-glucaric acid pathway.
12
13
14

15 220 To simulate a lean medium that might be obtained from the hydrolysis of lignocellulosic
16
17 221 biomass, the $\Delta pgi \Delta zwf$ strain was also tested in a modified MOPS minimal medium containing
18
19 222 10 g/L D-glucose and 6 g/L L-arabinose. Although the strain grew more slowly under these
20
21 223 conditions, D-glucaric acid titers of 0.40 ± 0.02 g/L were obtained, nearly as much as observed
22
23 224 in supplemented LB (Figure 5). The yield of D-glucaric acid from glucose was 47%; however,
24
25 225 approximately 0.2 g/L of *myo*-inositol was also produced, bringing the total yield of G6P-derived
26
27 226 products to 71%. *Myo*-inositol is produced from G6P as an intermediate during D-glucaric acid
28
29 227 production and has previously been observed to build up in the culture medium under some
30
31 228 conditions (Moon et al., 2009). Modified MOPS medium containing D-xylose and D-glucose
32
33 229 was also tested, but no growth of the $\Delta pgi \Delta zwf$ mutant was observed, possibly due to stronger
34
35 230 residual catabolite repression of *xyLAB* in minimal medium. **In modified MOPS medium
36
37 231 supplemented with D-xylose alone, M6 does not produce glucaric acid or *myo*-inositol,
38
39 232 consistent with the expectation that glucaric acid can only be derived from glucose in a Δpgi
40
41 233 Δzwf mutant (Supplementary Table 1).**
42
43
44
45
46
47

48 234 **4. Discussion**

49
50 235 Traditionally, the main focus of metabolic engineering projects has been on increasing the
51
52 236 final titer of a product of interest, and this approach has been widely successful for high-value
53
54 237 compounds such as pharmaceutical intermediates and therapeutic proteins. However, increasing
55
56
57
58
59
60

1
2
3 238 titers alone may not be sufficient for low-margin, high-volume bioproducts such as commodity
4
5 239 chemicals. In these cases, product yield becomes an important process consideration, as raw
6
7
8 240 material costs can be a large percentage of the manufacturing costs. Strategies which are able to
9
10 241 increase product yield without sacrificing titer would be valuable tools for the metabolic
11
12 242 engineer.

13
14
15 243 The use of renewable feedstocks such as lignocellulosic biomass for biochemical production
16
17 244 presents an interesting opportunity for increasing the yield of biochemicals derived directly from
18
19
20 245 glucose: in addition to glucose, lignocellulosic biomass contains several other fermentable sugars
21
22 246 (e.g., xylose and arabinose) which may be used for biomass formation while reserving glucose
23
24 247 solely for product generation. Because wild-type *E. coli* preferentially consumes glucose, strain
25
26 248 engineering is necessary to shift the cell's preference towards alternative carbon sources. In this
27
28 249 work, we characterized the carbon source preference of a $\Delta pgi \Delta zwf$ mutant and explored its
29
30 250 ability to improve the yield of D-glucaric acid on D-glucose.

31
32
33
34 251 As expected, deletion of *pgi* and *zwf* eliminates the cell's ability to consume D-glucose for
35
36 252 biomass formation. Catabolite repression is eliminated in this strain as well, as the $\Delta pgi \Delta zwf$
37
38 253 mutant is able to consume L-arabinose, glycerol, and D-xylose in the presence of D-glucose.
39
40 254 Because glucose-mediated catabolite repression occurs when glucose transport into the cell is
41
42 255 high, we believe that intracellular buildup of glucose-6-phosphate in the $\Delta pgi \Delta zwf$ mutant leads
43
44 256 to significantly reduced glucose transport, alleviating catabolite repression. Interestingly,
45
46 257 introduction of the D-glucaric acid pathway, which should draw down intracellular glucose-6-
47
48 258 phosphate pools, does not appear to affect the uptake of alternative carbon sources in the
49
50
51 259 presence of D-glucose. We speculate that glucose influx in the presence of INO1 is not high
52
53 260 enough to significantly reduce the levels of phosphorylated EIIA^{Glc} to result in activation of
54
55
56
57
58
59
60

1
2
3 261 catabolite repression. Because the threshold rate of glucose import necessary for activation of
4
5 262 catabolite repression is unknown, efforts to further increase the activity of INO1 or to introduce
6
7
8 263 more active glucose consumption pathways should proceed with caution to avoid reactivation of
9
10
11 264 catabolite repression.

12 13 265 **5. Conclusions**

14
15 266 In this work, we investigate the behavior of a $\Delta pgi \Delta zwf$ mutant and its ability to utilize
16
17 267 alternative carbon sources for cell growth while reserving D-glucose for product formation. This
18
19
20 268 strain was able to consume L-arabinose, glycerol, and D-xylose even in the presence of D-
21
22 269 glucose, and yields of D-glucaric acid on D-glucose were increased 9- to 18-fold in the Δpgi
23
24
25 270 Δzwf strain. Additionally, product titers were also increased, as the initial D-glucaric acid
26
27 271 pathway enzyme was no longer in competition with glycolytic enzymes for glucose-6-phosphate.
28
29 272 Furthermore, the $\Delta pgi \Delta zwf$ mutant exhibits similar yield increases in minimal medium,
30
31 273 suggesting the strain's potential in an industrial setting; however, additional investigation is
32
33
34 274 necessary to fully characterize the strain's robustness. These gains in product yield should easily
35
36 275 translate to other bioproducts derived from D-glucose, and it is hoped that this strain will help
37
38
39 276 improve the process economics of these value-added biochemicals.

40 41 277 **6. Acknowledgements**

42
43 278 This work was supported by the National Science Foundation through the Synthetic Biology
44
45 279 Engineering Research Center (E.S., Grant No. EEC-0540879) and the CAREER Award program
46
47
48 280 (I.M.B., Grant No. CBET- 0954986), and through the Biotechnology Training Program of the
49
50
51 281 National Institutes of Health (I.M.B., Grant No. T32GM008334).

52
53 282
54
55
56 283
57
58
59
60

284 **References**

- 285 Amann E, Brosius J. 1985. "ATG vectors" for regulated high-level expression of cloned genes in
286 Escherichia coli. *Gene*. **40**:183–190.
- 287 Baba T, Ara T, Hasegawa M, Takai Y, Okumura Y, Baba M, Datsenko KA, Tomita M, Wanner
288 BL, Mori H. 2006. Construction of Escherichia coli K-12 in-frame, single-gene knockout
289 mutants: the Keio collection. *Mol. Syst. Biol.* **2**:2006.0008.
- 290 Balderas-Hernández VE, Hernández-Montalvo V, Bolívar F, Gosset G, Martínez A. 2011.
291 Adaptive evolution of Escherichia coli inactivated in the phosphotransferase system operon
292 improves co-utilization of xylose and glucose under anaerobic conditions. *Appl. Biochem.*
293 *Biotechnol.* **163**:485–496.
- 294 Chassagnole C, Noisommit-Rizzi N, Schmid JW, Mauch K, Reuss M. 2002. Dynamic modeling
295 of the central carbon metabolism of Escherichia coli. *Biotechnol. Bioeng.* **79**:53–73.
296 <http://doi.wiley.com/10.1002/bit.10288>.
- 297 Curran KA, Alper H. 2012. Expanding the chemical palate of cells by combining systems
298 biology and metabolic engineering. *Metab. Eng.* **14**:289–297.
- 299 Datsenko KA, Wanner BL. 2000. One-step inactivation of chromosomal genes in Escherichia
300 coli K-12 using PCR products. *Proc. Natl. Acad. Sci. U.S.A* **97**:6640–6645.
- 301 Gonçalves GAL, Prazeres DMF, Monteiro GA, Prather KLJ. 2013. De novo creation of
302 MG1655-derived E. coli strains specifically designed for plasmid DNA production. *Appl.*
303 *Microbiol. Biotechnol.* **97**:611–620.

- 1
2
3 304 Hernández-Montalvo V, Martínez A, Hernández-Chavez G, Bolivar F, Valle F, Gosset G. 2003.
4
5
6 305 Expression of galP and glk in a Escherichia coli PTS mutant restores glucose transport and
7
8 306 increases glycolytic flux to fermentation products. *Biotechnol. Bio* **83**:687–694.
9
10
11 307 Johnson DT, Taconi KA. 2009. The glycerin glut: options for the value-added conversion of
12
13 308 crude glycerol resulting from biodiesel production. *Environ. Prog.* **26**:338–348.
14
15
16
17 309 Joyce BL, Stewart CN. 2012. Designing the perfect plant feedstock for biofuel production: using
18
19 310 the whole buffalo to diversify fuels and products. *Biotechnol. Adv.* **30**:1011–1022.
20
21
22
23 311 Kogure T, Wakisaka N, Takaku H, Takagi M. 2007. Efficient production of 2-deoxy-scylo-
24
25 312 inosose from D-glucose by metabolically engineered recombinant Escherichia coli. *J.*
26
27 313 *Biotechnol* **129**:502–509.
28
29
30
31 314 Lee SY. 1996. Bacterial Polyhydroxyalkanoates **49**:1–14.
32
33
34
35 315 Moon TS, Yoon SH, Lanza AM, Roy-Mayhew JD, Prather KLJ. 2009. Production of glucaric
36
37 316 acid from a synthetic pathway in recombinant Escherichia coli. *Appl. Environ. Microbiol.*
38
39 317 **75**:589–595.
40
41
42
43 318 Pandey RP, Malla S, Simkhada D, Kim BG, Sohng JK. 2013. Production of 3-o-xylosyl
44
45 319 quercetin in Escherichia coli. *Appl. Microbiol. Biotechnol.* **97**:1889–1901.
46
47
48
49 320 Roe AJ, Mclaggan D, Davidson IAN, Byrne CO, Booth IR, Laggan DMC, Davidson IAN. 1998.
50
51 321 Perturbation of anion balance during inhibition of growth of Escherichia coli by weak acids.
52
53 322 *J. Bacteriol.* **180**:767–772.
54
55
56
57
58
59
60

- 1
2
3 323 Rogers P, Chen J, Zidwick MJO. 2006. The Prokaryotes. New York, NY: Springer New York.
4
5
6 324 <http://www.springerlink.com/index/10.1007/0-387-30741-9>.
7
8
9 325 Sambrook J, Russell DW. 2001. Molecular Cloning: A Laboratory Manual. Cold Spring Harbor
10
11 326 Laboratory Press, Cold Spring Harbor.
- 12
13
14
15 327 Shiue E, Prather KLJ. 2014. Improving D-glucaric acid production from myo-inositol in E. coli
16
17 328 by increasing MIOX stability and myo-inositol transport. *Metab. Eng.* **22**:22–31.
- 18
19
20
21 329 Solomon K V, Moon TS, Ma B, Sanders TM, Prather KLJ. 2013. Tuning primary metabolism
22
23 330 for heterologous pathway productivity. *ACS Synth. Biol.* **2**:126–135.
- 24
25
26
27 331 Wang D, Li Q, Yang M, Zhang Y, Su Z, Xing J. 2011. Efficient production of succinic acid from
28
29 332 corn stalk hydrolysates by a recombinant Escherichia coli with ptsG mutation. *Process*
30
31 333 *Biochem.* **46**:365–371.
- 32
33
34
35 334 Werpy T, Petersen G. 2004. Top value added chemicals from biomass, volume 1: results of
36
37 335 screening for potential candidates from sugars and synthesis gas. *U. S. Dep. Energy*. U.S.
38
39 336 Department of Energy, Washington, DC.
- 40
41
42
43 337 Yoon SH, Moon TS, Iranpour P, Lanza AM, Prather KLJ. 2009. Cloning and characterization of
44
45 338 uronate dehydrogenases from two pseudomonads and Agrobacterium tumefaciens strain
46
47
48 339 C58. *J. Bacteriol.* **191**:1565–1573.
49
50
51
52
53
54
55
56
57
58
59
60

Table I: *E. coli* strains, plasmids, and oligonucleotides used

Name	Relevant Genotype	Reference
Strains		
DH10B	F ⁻ <i>mcrA</i> Δ (<i>mrr-hsdRMS-mcrBC</i>) ϕ 80 <i>lacZ</i> Δ M15 Δ <i>lacX74</i> <i>recA1</i> <i>endA1</i> <i>araD139</i> Δ (<i>ara</i> , <i>leu</i>)7697 <i>galU</i> <i>galK</i> λ - <i>rpsL</i> <i>nupG</i>	Life Technologies (Carlsbad, CA)
JW1841-1	F ⁻ , Δ (<i>araD-araB</i>)567, Δ <i>lacZ</i> 4787(:: <i>rrnB-3</i>), λ ⁻ , Δ <i>zwf</i> -777:: <i>kan</i> , <i>rph-1</i> , Δ (<i>rhaD-rhaB</i>)568, <i>hsdR</i> 514	CGSC #9537 (Baba et al., 2006)
MG1655	F ⁻ λ <i>ilvG</i> <i>frb</i> - 50 <i>rph-1</i>	ATCC #700926
M2	MG1655(DE3) Δ <i>endA</i> Δ <i>recA</i>	(Shiue and Prather, 2014)
M2-2	MG1655(DE3) Δ <i>endA</i> Δ <i>recA</i> Δ <i>gudD</i> Δ <i>uxaC</i>	(Shiue and Prather, 2014)
M3	MG1655 Δ <i>endA</i> Δ <i>recA</i> Δ <i>pgi</i>	(Gonçalves et al., 2013)
M4	MG1655(DE3) Δ <i>endA</i> Δ <i>recA</i> Δ <i>pgi</i> Δ <i>zwf</i>	This study
M5	MG1655(DE3) Δ <i>endA</i> Δ <i>recA</i> Δ <i>pgi</i> Δ <i>zwf</i> Δ <i>uxaC</i>	This study
M6	MG1655(DE3) Δ <i>endA</i> Δ <i>recA</i> Δ <i>pgi</i> Δ <i>zwf</i> Δ <i>uxaC</i> Δ <i>gudD</i>	This study
Plasmids		
pCP20	Rep ^a , Amp ^R , Cm ^R , FLP recombinase expressed by λ <i>p_r</i> under control of λ cI857	CGSC #7629
pKD13	R6K γ <i>ori</i> , Amp ^R , <i>kan</i>	CGSC #7633
pKD46	R101 <i>ori</i> , <i>repA101</i> ^a , Amp ^R , <i>araC</i> , <i>araBp</i> - λ _{γ} - λ _{β} - λ _{exo}	CGSC #7739
pKD46recA	R101 <i>ori</i> , <i>repA101</i> ^a , Amp ^R , <i>araC</i> , <i>araBp</i> - λ _{γ} - λ _{β} - λ _{exo} , <i>recA</i>	(Solomon et al., 2013)
pRSFDuet-1	pRSR1030 <i>ori</i> , <i>lacI</i> , Kan ^R	EMD4 Biosciences (Darmstadt, Germany)
pTrc99A	pBR322 <i>ori</i> , Amp ^R	(Amann and Brosius, 1985)
pRSFD-IN	pRSFDuet-1 with INO1 inserted into the EcoRI and HindIII sites	(Moon et al., 2009)
pTrc-Udh	pTrc99A with Udh from <i>Pseudomonas syringae</i> inserted into the NcoI and HindIII sites	(Moon et al., 2009; Yoon et al., 2009)
pRSFD-IN-Udh	pRSFD-IN with Udh inserted into the MfeI and XhoI sites	This study
pTrc-SUMO-MIOX	pTrc99A with SUMO-MIOX	(Shiue and Prather, 2014)

Oligonucleotides

pKD13_gudD_fwd

pKD13_gudD_rev

pKD13_uxaC_fwd

pKD13_uxaC_rev

^a All oligonucleotides purchased from Sigma-Genosys (St. Louis, MO). Homologous sequences used for recombination are underlined.

For Peer Review

Table II: Maximum growth rates of various strains in rich medium supplemented with various carbon sources.

Strain *	Alternative Carbon Source	Glucose	μ_{\max} (hr ⁻¹)
M2	L-Arabinose	-	1.00 ± 0.01
		+	1.01 ± 0.06
	Glycerol	-	0.98 ± 0.02
		+	0.97 ± 0.04
	D-Xylose	-	1.00 ± 0.03
		+	0.87 ± 0.20
M4	L-Arabinose	-	0.65 ± 0.01
		+	0.66 ± 0.02
	Glycerol	-	0.66 ± 0.05
		+	0.68 ± 0.01
	D-Xylose	-	0.70 ± 0.01
		+	0.67 ± 0.01

* **M2:** MG1655(DE3) $\Delta endA \Delta recA$; **M4:** MG1655(DE3) $\Delta endA \Delta recA \Delta pgi \Delta zwf$

Table III: D-glucaric acid yields on D-glucose for various carbon sources.

Strain *	Carbon	D-Glucaric Acid Titer (g/L)	Yield on D-Glucose (g/g)
M2-2	L-Arabinose in LB	0.13 ± 0.01	0.044 ± 0.002
	Glycerol in LB	0.20 ± 0.02	0.052 ± 0.009
	D-Xylose in LB	0.13 ± 0.01	0.039 ± 0.002
M6	L-Arabinose in LB	0.50 ± 0.01	0.76 ± 0.13
	Glycerol in LB	0.81 ± 0.10	0.44 ± 0.04
	D-Xylose in LB	1.19 ± 0.08	0.73 ± 0.03
	L-Arabinose in MOPS	0.40 ± 0.02	0.47 ± 0.25

* **M2-2:** MG1655(DE3) $\Delta endA \Delta recA \Delta gudD \Delta luxaC$; **M6:** MG1655(DE3) $\Delta endA \Delta recA \Delta pgi \Delta zwf \Delta luxaC \Delta gudD$

Figures

Figure 1: Glucose utilization pathways in *E. coli*.

Figure 2: Growth curves for strains M2 (top row) and M4 (bottom row) in rich medium supplemented with L-arabinose (“Ara”, triangles), glycerol (“Gly”, circles), and D-xylose (“Xyl”, squares) with D-glucose (“Glc”) absent (open points) or present (filled points). M2: MG1655(DE3) $\Delta endA recA$; M4: MG1655(DE3) $\Delta endA \Delta recA \Delta pgi \Delta zwf$.

Figure 3: Carbon source and acetate (“Act”, circles) concentrations in rich medium cultures of M2 (filled points, solid line) and M4 (open points, dotted lines) supplemented with L-arabinose (“Ara”, triangles), glycerol (“Gly”, inverted triangles), and D-xylose (“Xyl”, diamonds) with D-glucose (“Glc”, squares) absent (left column) or present (right column). M2: MG1655(DE3) $\Delta endA \Delta recA$; M4: MG1655(DE3) $\Delta endA \Delta recA \Delta pgi \Delta zwf$.

Figure 4: D-glucaric acid production (“Gla”, circles) from D-glucose in strains M2-2 and M6 in rich medium. Cultures contained strain M2-2 or M6 harboring pRSFD-IN-Udh and pTrc-SUMO-MIOX and were grown in LB supplemented with D-glucose (“Glc”, squares) and L-arabinose (“Ara”, triangles), glycerol (“Gly”, inverted triangles), or D-xylose (“Xyl”, diamonds). M2-2: MG1655(DE3) $\Delta endA \Delta recA \Delta gudD \Delta auxaC$ (filled points, solid line); M6: MG1655(DE3) $\Delta endA \Delta recA \Delta gudD \Delta auxaC \Delta pgi \Delta zwf$ (open points, dotted line).

1
2
3 **Figure 5:** Growth and D-glucaric acid (“Gla”, circles) production from D-glucose in strain M6
4 in lean medium. Cultures contained M6 harboring pRSFD-IN-Udh and pTrc-SUMO-MIOX and
5 were grown in modified MOPS minimal medium supplemented with 6 g/L L-arabinose (“Ara”,
6 triangles) and 10 g/L D-glucose (“Glc”, squares). M6: MG1655(DE3) $\Delta endA \Delta recA \Delta gudD$
7
8
9
10
11
12
13 *\Delta luxaC \Delta pgi \Delta zwf*.
14
15
16

17 **Graphical TOC:** Knockout of *pgi* and *zwf* from *E. coli* prevents the cell from using glucose for
18 biomass production, allowing the carbon to be diverted towards bioproducts of interest (e.g., D-
19 glucaric acid). Alternative carbon sources (e.g., D-xylose, glycerol, and L-arabinose), which may
20 be derived from biomass hydrolysis, can be fed for biomass formation.
21
22
23
24
25
26
27
28
29
30
31
32
33
34
35
36
37
38
39
40
41
42
43
44
45
46
47
48
49
50
51
52
53
54
55
56
57
58
59
60

Figure 1

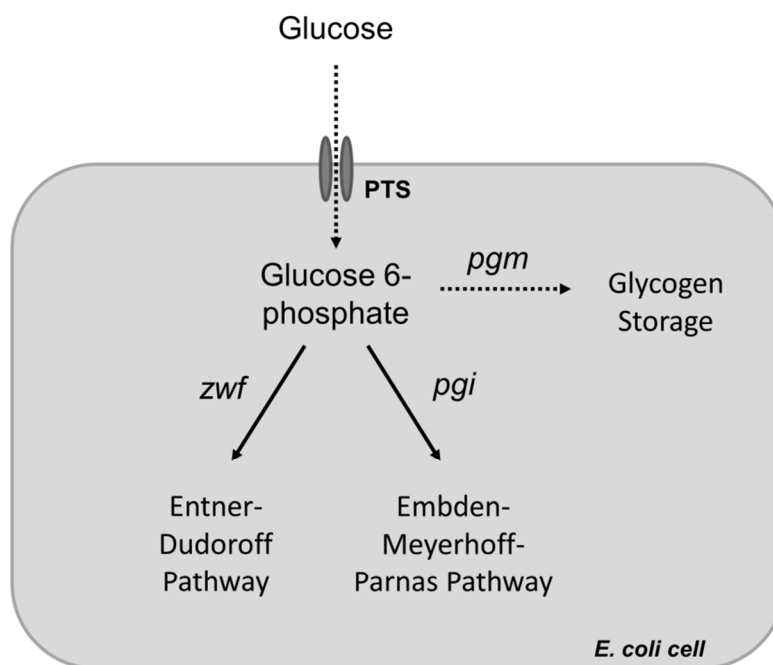
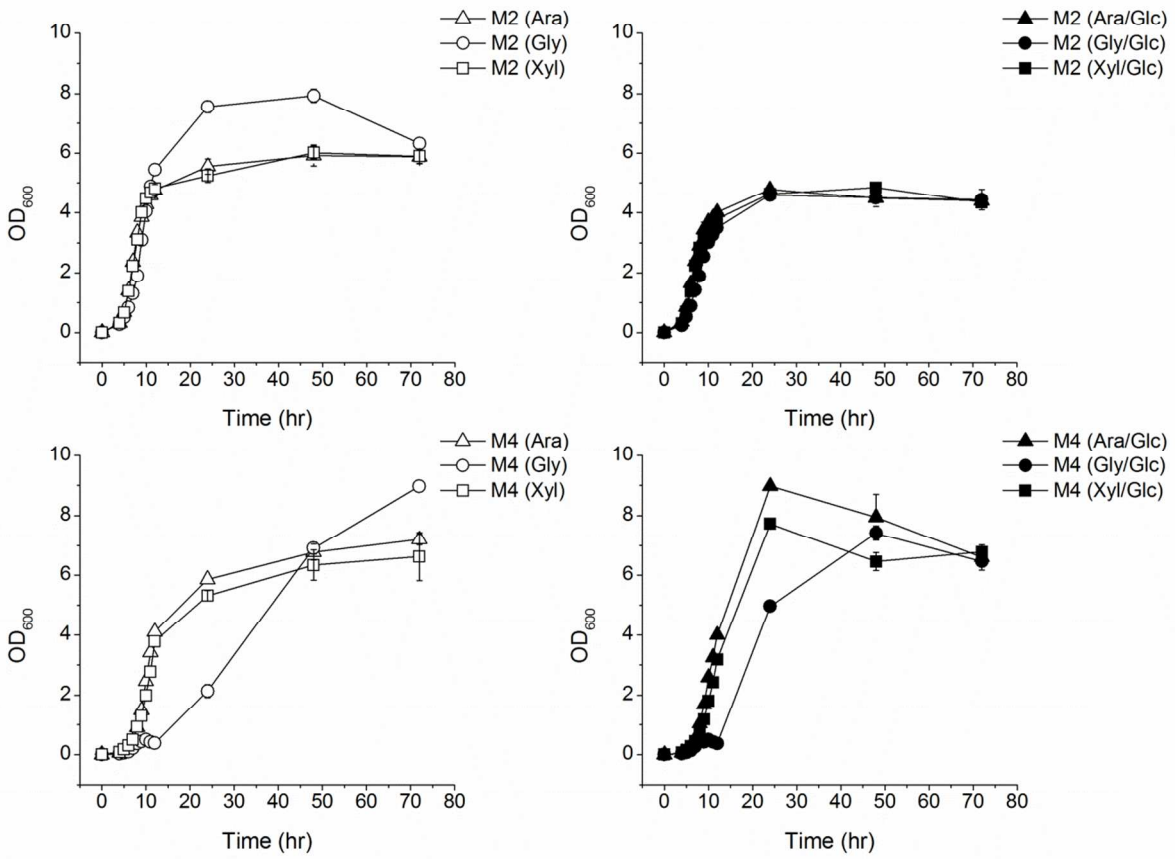


Figure 2



view

Figure 3

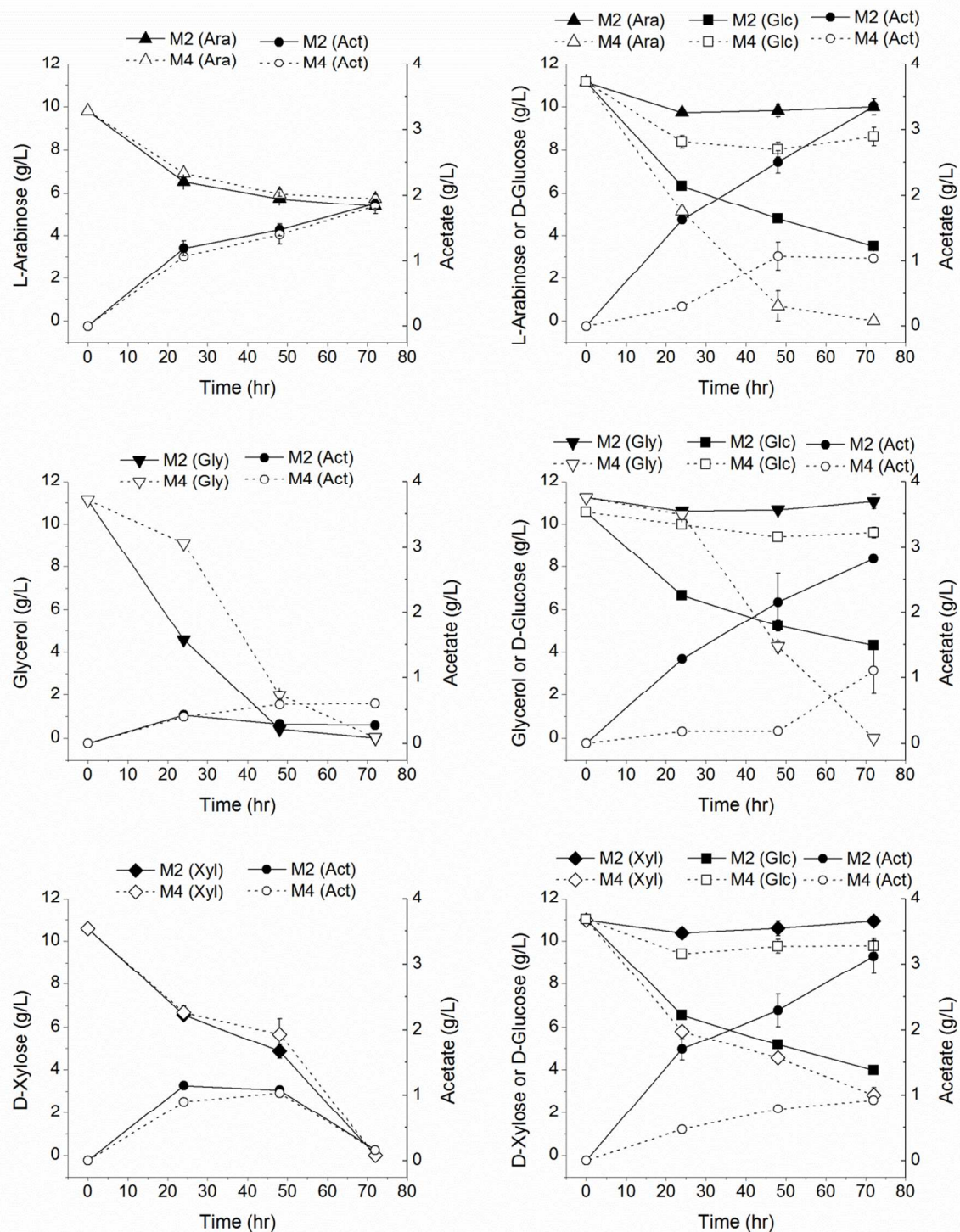


Figure 4

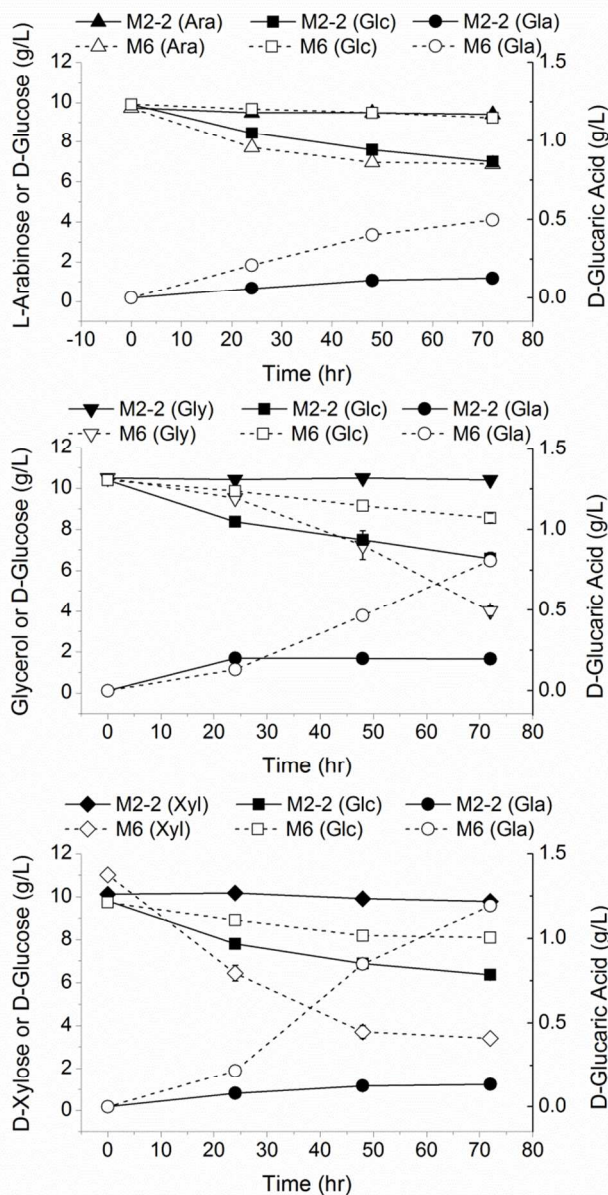
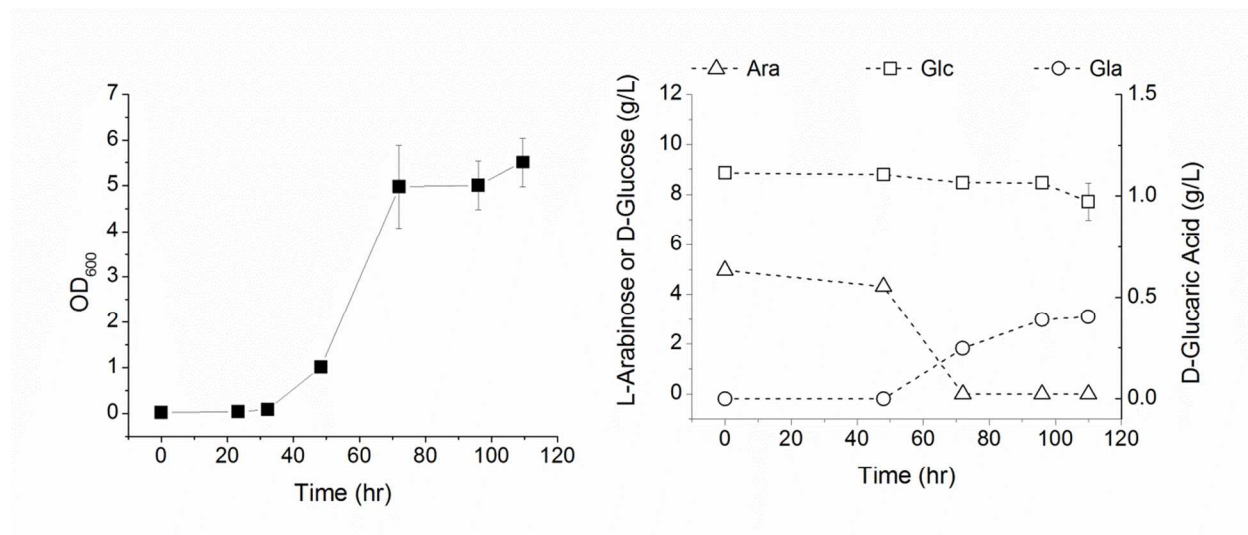
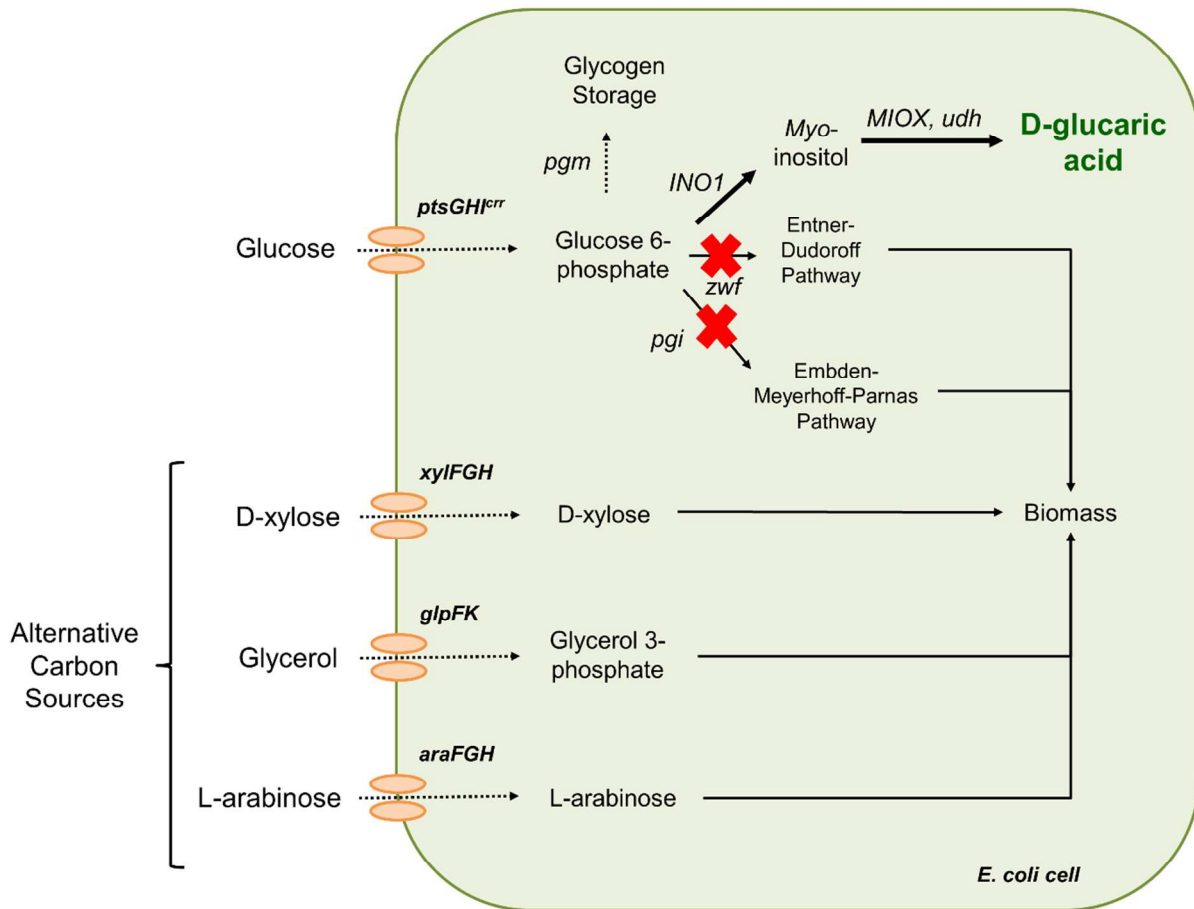


Figure 5



Peer Review

Graphical TOC



view

1
2
3
4
5
6
7
8
9
10
11
12
13
14
15
16
17
18
19
20
21
22
23
24
25
26
27
28
29
30
31
32
33
34
35
36
37
38
39
40
41
42
43
44
45
46
47
48
49
50
51
52
53
54
55
56
57
58
59
60

Table I: *E. coli* strains, plasmids, and oligonucleotides used

Name	Relevant Genotype	Reference
Strains		
DH10B	<i>F⁻ mcrA Δ(mrr-hsdRMS-mcrBC) φ80lacZΔM15 ΔlacX74 recA1 endA1 araD139 Δ(ara, leu)7697 galU galK λ-rpsL nupG</i>	Life Technologies (Carlsbad, CA)
JW1841-1	<i>F⁻, Δ(araD-araB)567, ΔlacZ4787(::rrnB-3), λ⁻, Δzwf-777::kan, rph-1, Δ(rhaD-rhaB)568, hsdR514</i>	CGSC #9537 (Baba et al., 2006)
MG1655	<i>F⁻ λ ilvG⁻ frb-50 rph-1</i>	ATCC #700926
M2	<i>MG1655(DE3) ΔendA ΔrecA</i>	(Shiue and Prather, 2014)
M2-2	<i>MG1655(DE3) ΔendA ΔrecA ΔgudD ΔuxaC</i>	(Shiue and Prather, 2014)
M3	<i>MG1655 ΔendA ΔrecA Δpgi</i>	(Gonçalves et al., 2013)
M4	<i>MG1655(DE3) ΔendA ΔrecA Δpgi Δzwf</i>	This study
M5	<i>MG1655(DE3) ΔendA ΔrecA Δpgi Δzwf ΔuxaC</i>	This study
M6	<i>MG1655(DE3) ΔendA ΔrecA Δpgi Δzwf ΔuxaC ΔgudD</i>	This study
Plasmids		
pCP20	<i>Rep^a, Amp^R, Cm^R, FLP recombinase expressed by λ p_r under control of λ cI857</i>	CGSC #7629
pKD13	<i>R6Kγ ori, Amp^R, kan</i>	CGSC #7633

1			
2			
3	pKD46	R101 <i>ori</i> , <i>repA101</i> ^a , Amp ^R , <i>araC</i> , <i>araBp-λ_γ-λ_β-λ_{exo}</i>	CGSC #7739
4			
5	pKD46recA	R101 <i>ori</i> , <i>repA101</i> ^a , Amp ^R , <i>araC</i> , <i>araBp-λ_γ-λ_β-λ_{exo}</i> , <i>recA</i>	(Solomon et al., 2013)
6			
7	pRSFDuet-1	pRSR1030 <i>ori</i> , <i>lacI</i> , Kan ^R	EMD4 Biosciences (Darmstadt, Germany)
8			
9			
10			
11	pTrc99A	pBR322 <i>ori</i> , Amp ^R	(Amann and Brosius, 1985)
12			
13	pRSFD-IN	pRSFDuet-1 with INO1 inserted into the EcoRI and HindIII sites	(Moon et al., 2009)
14			
15	pTrc-Udh	pTrc99A with Udh from <i>Pseudomonas syringae</i> inserted into the NcoI and HindIII sites	(Moon et al., 2009; Yoon et al., 2009)
16			
17			
18			
19	pRSFD-IN-Udh	pRSFD-IN with Udh inserted into the MfeI and XhoI sites	This study
20			
21	pTrc-SUMO-MIOX	pTrc99A with SUMO-MIOX	(Shiue and Prather, 2014)
22			
23			
24			
25			

Oligonucleotides5' → 3' Sequence^a

26			
27			
28	pKD13_gudD_fwd	<u>TCCCCGGCTGGACCTTTGACCGTAAACGTC</u> <u>CCCGTTTTTCGGCCGTCATTGATTCTGAAAAAG</u>	
29		<u>GACATAAATCTGTCAAACATGAGAATTAATTCC</u>	
30			
31			
32	pKD13_gudD_rev	<u>CAACAGGCTATTTTGC</u> <u>GTTTAGCATCAGTCTCAAACCGGCTCCAGATAGAGCCGGTTTTGG</u>	
33		<u>TTTTCTGTCGTGTAGGCTGGAGCTGCTTC</u>	
34			
35			
36	pKD13_uxaC_fwd	<u>AATTGGTGTGATAACTTTGTCAGCATCGCACCATAAAGCAAGCTAGCTCACTCGTTGAGAG</u>	
37		<u>GAAGACGAAACTGTCAAACATGAGAATTAATTCC</u>	
38			
39	pKD13_uxaC_rev	<u>AAATCTGCTAAAGCGACCGCGACGTTATCCAGCGCATGGATCTTGATGTATTGCATATCA</u>	
40		<u>ACCCAGACCGTGTAGGCTGGAGCTGCTTC</u>	
41			
42			

1
2
3
4
5
6
7
8
9
10
11
12
13
14
15
16
17
18
19
20
21
22
23
24
25
26
27
28
29
30
31
32
33
34
35
36
37
38
39
40
41
42
43
44
45
46
47
48
49

^a All oligonucleotides purchased from Sigma-Genosys (St. Louis, MO). Homologous sequences used for recombination are underlined.

For Peer Review

Table II: Maximum growth rates of various strains in rich medium supplemented with various carbon sources.

Strain *	Alternative Carbon Source	Glucose	μ_{\max} (hr ⁻¹)
M2	L-Arabinose	-	1.00 ± 0.01
		+	1.01 ± 0.06
	Glycerol	-	0.98 ± 0.02
		+	0.97 ± 0.04
	D-Xylose	-	1.00 ± 0.03
		+	0.87 ± 0.20
M4	L-Arabinose	-	0.65 ± 0.01
		+	0.66 ± 0.02
	Glycerol	-	0.66 ± 0.05
		+	0.68 ± 0.01
	D-Xylose	-	0.70 ± 0.01
		+	0.67 ± 0.01

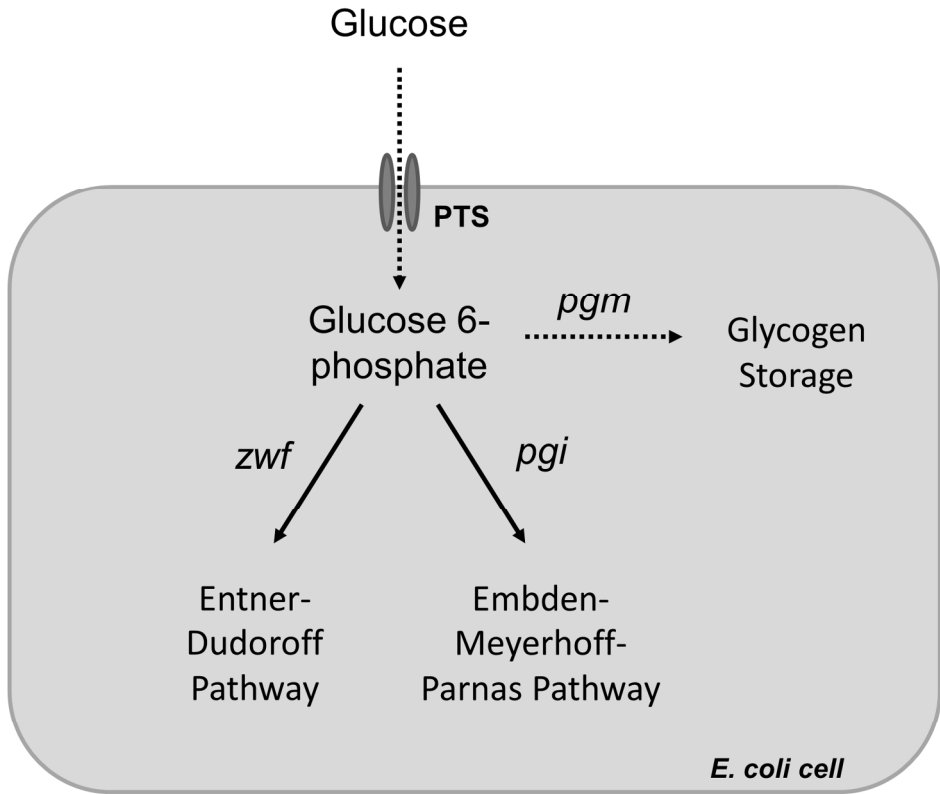
* **M2:** MG1655(DE3) $\Delta endA \Delta recA$; **M4:** MG1655(DE3) $\Delta endA \Delta recA \Delta pgi \Delta zwf$

Table III: D-glucaric acid yields on D-glucose for various carbon sources.

Strain *	Carbon	D-Glucaric Acid Titer (g/L)	Yield on D-Glucose (g/g)
M2-2	L-Arabinose in LB	0.13 ± 0.01	0.044 ± 0.002
	Glycerol in LB	0.20 ± 0.02	0.052 ± 0.009
	D-Xylose in LB	0.13 ± 0.01	0.039 ± 0.002
M6	L-Arabinose in LB	0.50 ± 0.01	0.76 ± 0.13
	Glycerol in LB	0.81 ± 0.10	0.44 ± 0.04
	D-Xylose in LB	1.19 ± 0.08	0.73 ± 0.03
	L-Arabinose in MOPS	0.40 ± 0.02	0.47 ± 0.25

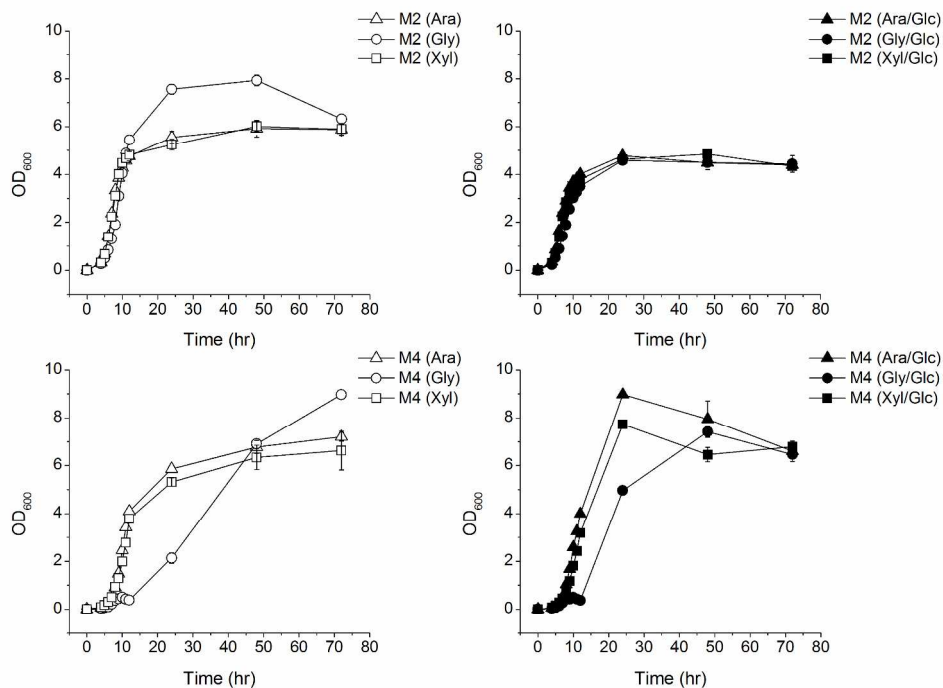
* **M2-2:** MG1655(DE3) Δ *endA* Δ *recA* Δ *gudD* Δ *luxaC*; **M6:** MG1655(DE3) Δ *endA* Δ *recA* Δ *pgi* Δ *zwf* Δ *luxaC* Δ *gudD*

1
2
3
4
5
6
7
8
9
10
11
12
13
14
15
16
17
18
19
20
21
22
23
24
25
26
27
28
29
30
31
32
33
34
35
36
37
38
39
40
41
42
43
44
45
46
47
48
49
50
51
52
53
54
55
56
57
58
59
60



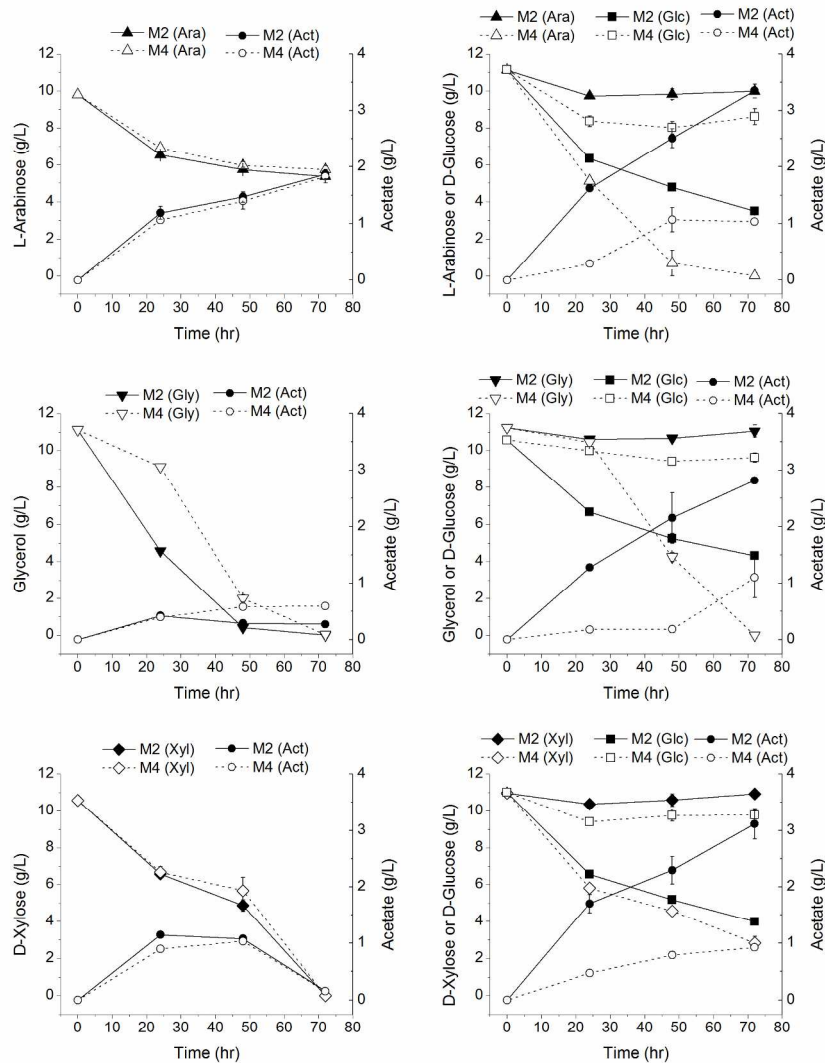
Glucose utilization pathways in *E. coli*
168x143mm (300 x 300 DPI)

view

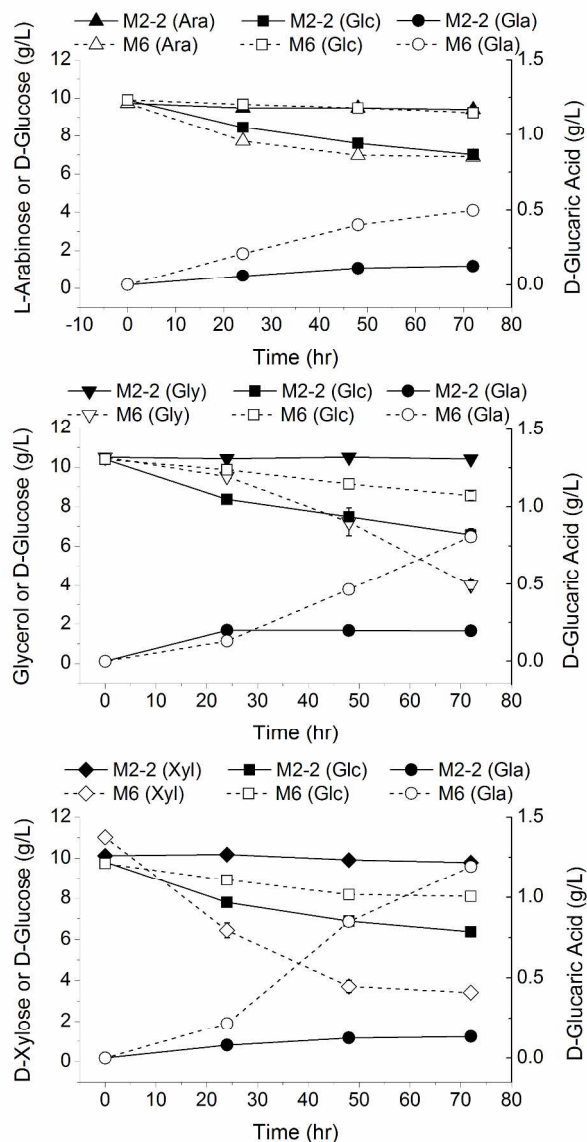


Growth curves for strains M2 (top row) and M4 (bottom row) in rich medium supplemented with L-arabinose ("Ara", triangles), glycerol ("Gly", circles), and D-xylose ("Xyl", squares) with D-glucose ("Glc") absent (open points) or present (filled points). M2: MG1655(DE3) Δ endA recA; M4: MG1655(DE3) Δ endA Δ recA Δ pgi Δ zwf.
 271x203mm (300 x 300 DPI)

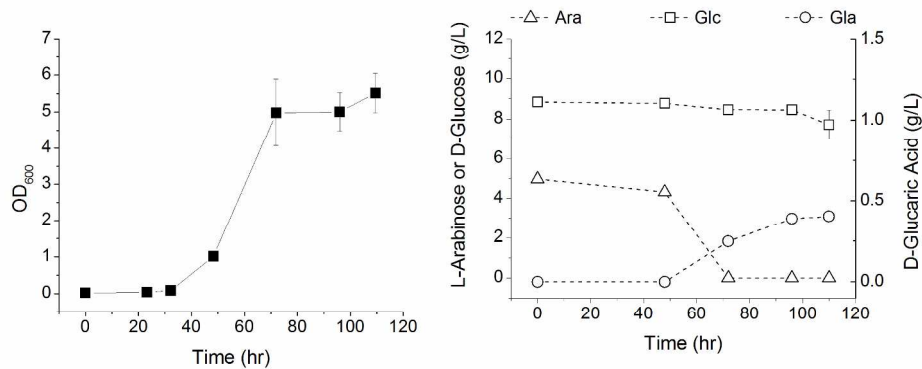
view



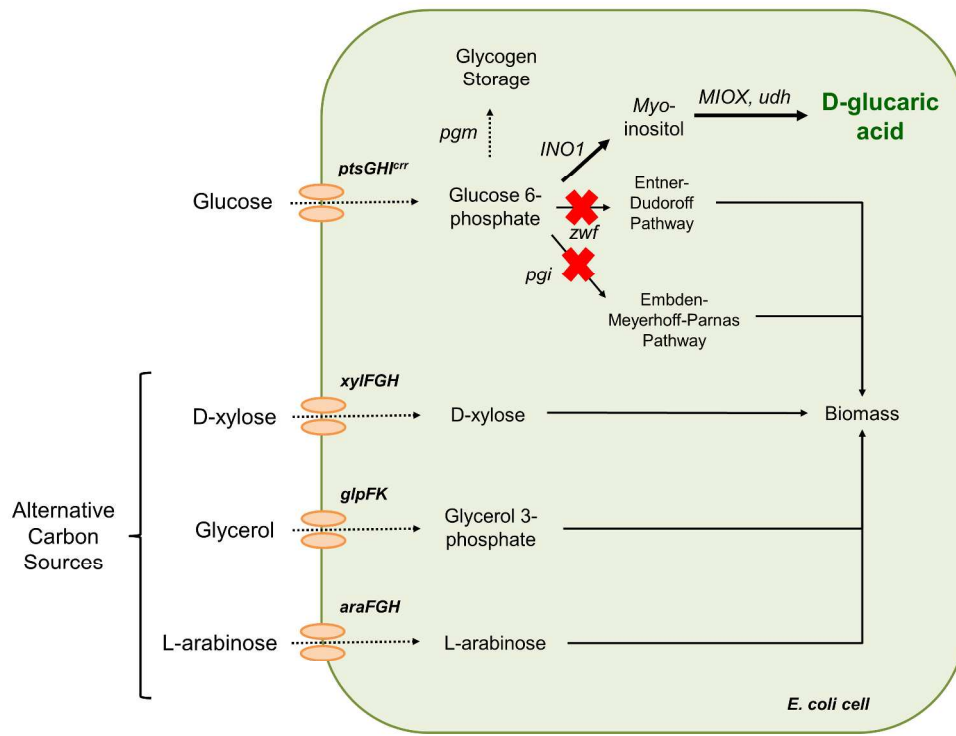
Carbon source and acetate ("Act", circles) concentrations in rich medium cultures of M2 (filled points, solid line) and M4 (open points, dotted lines) supplemented with L-arabinose ("Ara", triangles), glycerol ("Gly", inverted triangles), and D-xylose ("Xyl", diamonds) with D-glucose ("Glc", squares) absent (left column) or present (right column). M2: MG1655(DE3) Δ endA Δ recA; M4: MG1655(DE3) Δ endA Δ recA Δ pgi Δ zwf. 203x266mm (300 x 300 DPI)



D-glucaric acid production ("Gla", circles) from D-glucose in strains M2-2 and M6 in rich medium. Cultures contained strain M2-2 or M6 harboring pRSFD-IN-Udh and pTrc-SUMO-MIOX and were grown in LB supplemented with D-glucose ("Glc", squares) and L-arabinose ("Ara", triangles), glycerol ("Gly", inverted triangles), or D-xylose ("Xyl", diamonds). M2-2: MG1655(DE3) Δ endA Δ recA Δ gudD Δ uxaC (filled points, solid line); M6: MG1655(DE3) Δ endA Δ recA Δ gudD Δ uxaC Δ pgi Δ zwf (open points, dotted line).
178x341mm (300 x 300 DPI)



Growth and D-glucaric acid ("Gla", circles) production from D-glucose in strain M6 in lean medium. Cultures contained M6 harboring pRSFD-IN-Udh and pTrc-SUMO-MIOX and were grown in modified MOPS minimal medium supplemented with 6 g/L L-arabinose ("Ara", triangles) and 10 g/L D-glucose ("Glc", squares). M6: MG1655(DE3) Δ endA Δ recA Δ gudD Δ uxaC Δ pgi Δ zwf.
250x108mm (300 x 300 DPI)



Knockout of *pgi* and *zwf* from *E. coli* prevents the cell from using glucose for biomass production, allowing the carbon to be diverted towards bioproducts of interest (e.g., D-glucaric acid). Alternative carbon sources (e.g., D-xylose, glycerol, and L-arabinose), which may be derived from biomass hydrolysis, can be fed for biomass formation.

293x227mm (300 x 300 DPI)

1
2
3 **Supporting Information for *Improving Product Yields on D-Glucose in Escherichia coli via***
4 ***Knockout of *pgi* and *zwf* and Feeding of Supplemental Carbon Sources***
5
6
7

8 Eric Shiue, Irene M. Brockman, and Kristala L. J. Prather
9

10
11
12
13 Supplementary Methods
14

15 Supplementary Table 1: Glucaric acid production by M2-2 and M6 in modified MOPS minimal
16
17 medium with 10 g/L xylose
18

19
20 Supplementary Figure 1: Growth of strains M2 and M4 in M9 minimal medium supplemented
21
22 with D-glucose, D-xylose, or L-arabinose
23

24
25 Supplementary Figure 2: Growth of strains M2 and M4 on M9 agar supplemented with D-
26
27 glucose, D-xylose, or L-arabinose
28
29
30
31
32
33
34
35
36
37
38
39
40
41
42
43
44
45
46
47
48
49
50
51
52
53
54
55
56
57
58
59
60

Supplementary Methods

For glucaric acid production from xylose, cultures were grown in 250 mL baffled shake flasks containing a modified MOPS-buffered medium with 10 g/L D-xylose, 6 g/L NH₄Cl, 2 g/L K₂HPO₄, 2 mM MgSO₄, 0.1 mM CaCl₂, 40 mM MOPS, 4 mM tricine, 50 mM NaCl, 100 mM Bis-Tris, 134 μM EDTA, 31 μM FeCl₃, 6.2 μM ZnCl₃, 0.76 μM CuCl₂, 0.42 μM CoCl₂, 1.62 μM H₃BO₃, 0.081 μM MnCl₂, carbenicillin (100 μg/mL), and kanamycin (30 μg/ml). Seed cultures were started using a 1:100 dilution from LB and were grown at 30°C for 24 hours in modified MOPS. Working cultures were inoculated to an OD₆₀₀ of 0.02 and induced at inoculation with 0.05 mM IPTG. Cultures were incubated at 30°C, 250 rpm, and 80% relative humidity for 120 hours. Samples were taken periodically, centrifuged to remove cell debris, and the supernatants analyzed for metabolite concentrations by HPLC.

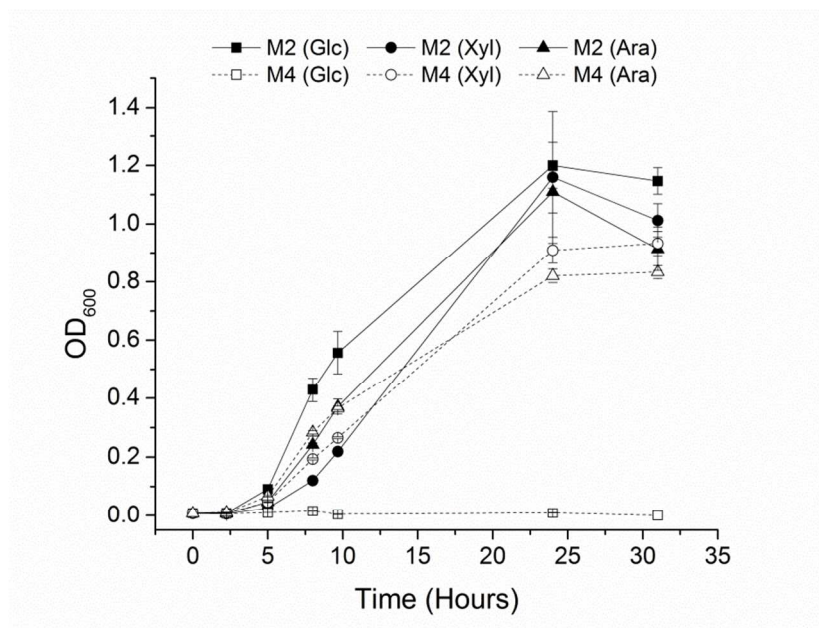
For growth measurements of M2 and M4, cultures were grown in M9 minimal medium supplemented with 4 g/L of the indicated carbon source (D-glucose, D-xylose, or L-arabinose). Seed cultures were started using a 1:100 dilution from LB into M9 with the appropriate carbon source. After growth at 37°C for 24 hours, these seed cultures were used to inoculate a working culture of M9 with the same carbon source for growth rate measurement. As the seed cultures for strain M4 did not grow in M9 + glucose, an M9 + xylose starter culture was used to seed the M9 + glucose culture for growth rate measurements. For growth on solid medium, M9 cultures at OD₆₀₀~0.2 were diluted 10³ or 10⁴ and 100 μl was plated on M9 agar with the same carbon source. For strain M4, a culture in M9 + xylose was used for dilution and plating on M9 glucose agar, as the strain did not grow in glucose minimal medium seed cultures.

Supplementary Table 1: Glucaric acid production by M2-2 and M6 harboring plasmids pTrc-SUMO-MIOX and pRSFD-IN-udh in modified MOPS minimal medium with 10 g/L xylose. Glucaric acid and *myo*-inositol production were not detected in M6, as expected due to the deletion of *pgi* and *zwf*, which prevents xylose flux toward glucose-6-phosphate. Peaks with retention time corresponding to the glucaric acid standard were observed in M2-2 cultures but were below the threshold for quantification. M2-2: MG1655(DE3) Δ *endA* Δ *recA* Δ *gudD* Δ *luxaC*; M6: MG1655(DE3) Δ *endA* Δ *recA* Δ *gudD* Δ *luxaC* Δ *pgi* Δ *zwf*.

	M2-2			M6		
	OD	glucaric acid (g/L)	<i>myo</i> -inositol (g/L)	OD	glucaric acid (g/L)	<i>myo</i> -inositol (g/L)
72 hours	2.2 ± 0.7	n.d.	n.d.	0.25 ± 0.01	n.d.	n.d.
120 hours	6.6 ± 0.2	< 0.1	0.025 ± 0.02	6.6 ± 0.2	n.d.	n.d.

n.d. = not detected

1
2
3
4 **Supplementary Figure 1:** Growth of M2 (filled symbols) and M4 (open symbols) in M9
5 minimal supplemented with D-glucose (“Glc”, squares), D-xylose (“Xyl”, circles), or L-
6 arabinose (“Ara”, triangles). M2: MG1655(DE3) $\Delta endA \Delta recA$; M4: MG1655(DE3) $\Delta endA$
7
8 $\Delta recA \Delta pgi \Delta zwf$.
9
10
11
12
13
14
15



1
2
3
4 **Supplementary Figure 2:** Growth of M2 and M4 on M9 agar supplemented with D-glucose, D-
5 xylose, or L-arabinose. (A) M9 agar plates after growth for 48 hours at 37° C. No growth was
6 observed for strain M4 on glucose. Carbon sources (left-right): D-glucose, D-xylose, L-
7 arabinose. Strain and dilution (top to bottom): M2 at 10⁴ dilution, M4 at 10⁴ dilution, M4 at 10³
8 dilution. (B) Closer view of M4 plates at 10³ dilution. Carbon source (left-right): D-glucose, D-
9 xylose, L-arabinose. M2: MG1655(DE3) $\Delta endA \Delta recA$; M4: MG1655(DE3) $\Delta endA \Delta recA \Delta pgi$
10 Δzwf .
11
12
13
14
15
16
17
18
19
20
21
22
23
24
25
26
27
28
29
30
31
32
33
34
35
36
37
38
39
40
41
42
43
44
45
46
47
48
49
50
51
52
53
54
55
56
57
58
59
60

